ACS OMEGA

Open Access

http://pubs.acs.org/journal/acsodf

Article

Ethidium Bromide Degradation by Cold Atmospheric Plasma in Water and the Assessment of Byproduct Toxicity for Environmental Protection

Reema Reema, Tejas Bedmutha, Nishanta Kakati, Veera Venkata Satya Prasanna Kumari Rayala, Pullapanthula Radhakrishnanand, Chingakham Juliya Devi, Debajit Thakur, and Kamatchi Sankaranarayanan*

Cite This: *ACS Omega* 2024, 9, 48044−48054

Read Online

ACCESS | Metrics & More | Article Recommendations | Supporting Information

ABSTRACT: Ethidium bromide (Et−Br) is a widely used fluorescent dye in molecular biology and biotechnology laboratories for visualizing nucleic acids in agarose gel electrophoresis. However, concerns have been raised about its environmental impact and potential health risks due to its persistence and toxicity. The potential accumulation and long-term effects on the environment necessitate the removal of Et−Br from water. This study investigates the potential of novel cold plasma technology for the degradation of Et−Br. Cold atmospheric plasma (CAP) is an environmentally friendly technology that does not produce secondary pollutants and generates a variety of potent chemical reactive oxidants such as hydroxyl radicals ($^{\bullet}OH$), H_2O_2, NO_2, and NO_3. In this study, Et−Br was treated with CAP for 15 min without the addition of any chemicals, resulting in substantial removal of Et−Br. The degradation kinetics revealed that the CAP-treated Et−Br followed a pseudo-first-order reaction, dependent on the treatment time of CAP. The degradation of Et−Br by CAP is distinctly evident through the results obtained from both high-performance liquid chromatography (HPLC) and liquid chromatography-mass spectrometry (LC-MS) analyses, providing clear evidence of the occurrence of degradation. Furthermore, toxicity analyses of the degradation products were conducted by evaluating the Et−Br intercalation ability with DNA before and after treatment of Et−Br with CAP. To supplement the assessment, the binding of Et−Br with BSA has also been studied before and after CAP treatment. The impact of CAP-treated Et−Br on the growth and colony-forming unit (CFU) counts of *Escherichia coli* was also evaluated. Results indicated an increase in bacterial growth with an increase in CAP treatment time, suggesting that the degradation products of Et−Br using CAP were nontoxic. This study highlights the potential of CAP as a clean and efficient technology for the degradation of Et−Br, presenting a promising solution for mitigating its environmental and health risks.

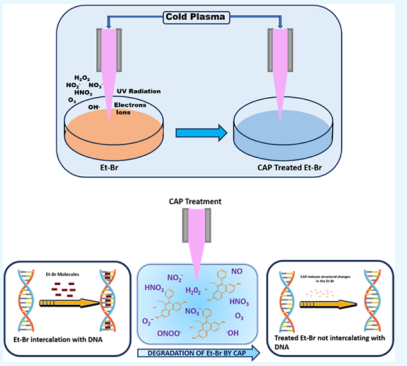

1. INTRODUCTION

Ethidium bromide (3,8-diamino-6-phenyl-5-ethylphenanthridinium bromide, Et−Br, Figure 1) is a potent mutagenic dye soluble in water, commonly used in molecular biology research for quick visualization of nucleic acids and deoxyribonucleic acid (DNA) in electrophoretic gels.[1] Et−Br is considered toxic due to its ability to intercalate with DNA and ribonucleic acid (RNA) molecules and can interfere with essential biological processes, such as DNA replication and transcription, leading to cellular dysfunction.[2,3] Prolonged exposure to Et−Br increases the risk of cancer development.[4,5] As it does not come under the regulation of the Environmental Protection Agency, it is generally poured down into the drains untreated, which has very toxic, cancer-causing, and mutagenic qualities.[6,7] When disposed of improperly, such as being

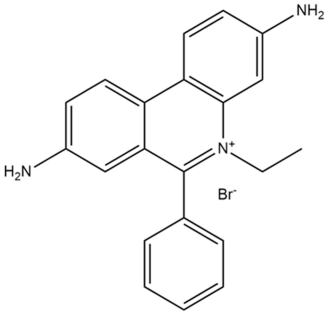

Figure 1. Chemical structure of ethidium bromide.

Received: May 6, 2024
Revised: October 17, 2024
Accepted: October 21, 2024
Published: November 25, 2024

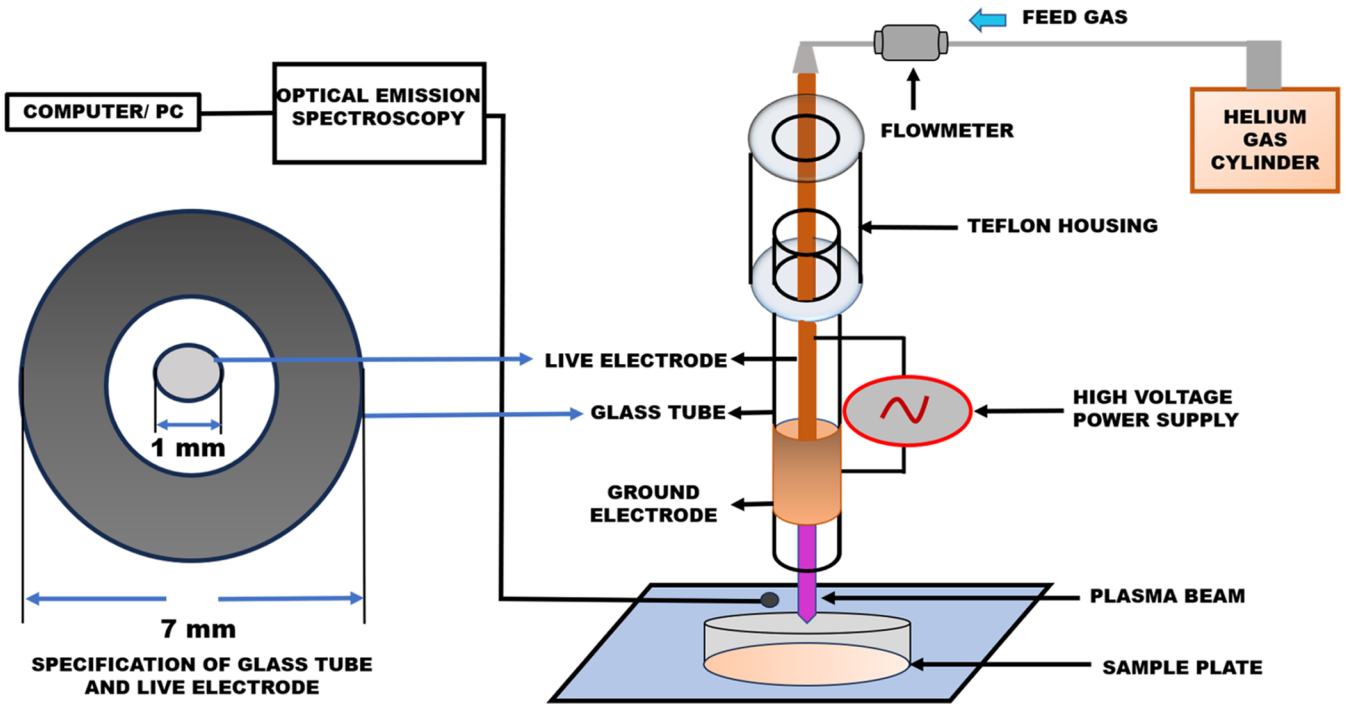

Figure 2. Lab setup of the cold atmospheric plasma jet and the optical emission spectrophotometer.

washed down laboratory sinks, it can enter wastewater systems and contaminate aquatic environments. Its persistence in the environment and potential bioaccumulation in aquatic organisms can have detrimental effects on ecosystems. Therefore, the treatment of water containing Et−Br is of utmost necessity.

There are many studies related to the treatment of polluted water with Et−Br such as chemical degradation including bleach treatment,[8] electrochemical degradation,[9−11] biological degradation by bacteria,[12] and catalysis;[13] but they all have drawbacks; degraded products generate other harmful secondary pollutants (waste) and require high chemical dosages to degrade. Also, irradiation techniques such as UV and γ radiation require higher dosages for significant removal.[14]

Cold atmospheric plasma (CAP) has emerged as a promising technological tool that has many applications in the wastewater treatment industry.[15−18] Many studies have been reported on CAP based degradation of hazardous chemicals mainly present in the environment, causing detrimental health effects .[19−23] The CAP is produced by providing high voltages between electrodes where an inert gas/mixture of gases is used to initiate ionization followed by the generation of many reactive species (ROS/RNS), UV photons, and electric field.[24−26] CAP in liquid and gas−liquid environments produces radicals, such as hydroxyl radicals, hydrogen peroxide, nitrate, nitrite, and nitric oxide, responsible for the degradation of chemicals in less treatment time with no addition of chemicals. All energetic species synergistically create a preferable oxidation environment for the degradation of hazardous chemicals.[27,28] Herein, a comprehensive study on the degradation of Et−Br using CAP has been investigated. The study of degradation kinetics has been done using UV−vis spectroscopy. Analytical techniques such as high-performance liquid chromatography (HPLC) and liquid chromatography−mass spectroscopy (LC-MS) have been employed to analyze the changes in Et−Br before and after treatment of Et−Br with CAP. Also, the effect of intercalation of Et−Br with DNA on the growth of *E. coli* was studied before and after CAP treatment to analyze its toxicity effects after degradation. Furthermore, an assessment of the toxicity of byproducts resulting from the degradation of Et−Br via CAP has been conducted to underscore the capability of CAP in effectively eliminating Et−Br without harming the environment.

2. MATERIAL AND METHODS

2.1. Materials and Reagents. Et−Br (product number: 18096DJ; CAS no. 1239/45/8; melting point: 260−262 °C; chemical formula $C_{21}H_{20}N_3$ Br; molecular weight: 394.2 g/mol) was purchased from Sigma Aldrich. A stock solution of Et−Br with a concentration of 50 μM was prepared for the experiments. Millipore water (resistance 18.2 MΩ) was used to prepare the samples. BSA, identified by Chemical Abstracts Service (CAS) numbers 9048-46-8, was obtained from Sigma Aldrich. Acetonitrile of HPLC grade from Sigma Aldrich was used to perform the HPLC experiment.

2.2. Experimental Plasma Setup and Its Characterization. The setup of the cold atmospheric plasma (CAP) jet, as illustrated in Figure 2, includes a power supply (Ionics Power Solution Pvt. Ltd.), an electrode housing, and a cylinder of carrier gas. The high-voltage AC power supply (0−20 kV, 25 kHz) is utilized to provide high voltages between the electrodes. Within the electrode housing, there is a cylindrical glass tube with inner and outer diameters of 3 and 7 mm, respectively. A 1 mm diameter stainless steel rod as the live electrode is inserted into the glass tube, and a copper wire strip is wrapped around the glass tube as the ground electrode. To ensure protection and insulation from high voltages, the glass tube is encased in a Teflon housing known for its high thermal stability and low thermal conductivity, providing effective high-temperature insulation. The Teflon housing is connected to the gas inlet, with helium gas chosen as the carrier gas for this

https://doi.org/10.1021/acsomega.4c04302
ACS Omega 2024, 9, 48044−48054

experiment due to its high thermal conductivity, reducing the breakdown voltage required for plasma discharge. The flow rate of helium gas is set at 1.5 slm (standard liters per minute) and can be adjusted using a variable area flowmeter (Cole Palmer). Upon applying a 6 kV peak-to-peak voltage between the electrodes, the helium gas becomes ionized, leading to the generation of plasma discharge. We use a Tektronix 6015A high-voltage probe to measure the peak-to-peak voltage, which is approximately 6 kV at 30 kHz. Additionally, an Agilent N2783B current probe is employed to measure the current at the powered electrode, which is around 15 mA. In our earlier work, we obtained emission spectra ranging from 200 to 900 nm for He gas using an optical emission spectrometer (Andor-SR-303i-A) and used the NIST atomic spectra database to identify and depict spectral line valuable insights into the emission characteristics of the helium plasma.[15] A 5 mL sample is placed in a Petri dish positioned just below the plasma discharge, with the live electrode's tip situated approximately 8 mm above the liquid sample surface. The plasma discharge interacts with nitrogen and oxygen species, leading to excitation, ionization, and dissociation of molecules by electron impact with the surrounding air, producing short- and long-lived reactive species, including the hydroxyl radical and hydrogen peroxide,[19] which are transferred to the sample beneath the plasma plume discharge, as depicted in Figure 2.

2.3. Degradation Kinetics and Fluorescence Study. In order to conduct the experiments and analyze the degradation kinetics and other treatment-related characteristics, a stock solution of Et−Br at a concentration of 50 μM was created. The ultimate concentration of the Et−Br solution was 10 μm. Following that, 5 mL of the Et−Br solution was applied to Petri plates for CAP treatment durations of 3, 5, 7, 10, and 13 min. Moreover, the values of absorbance were taken of each sample using UV−visible spectroscopy (Shimadzu UV-2550, USA) to study the degradation kinetics of Et−Br with CAP. A calibration curve comprising 11 distinct known concentrations of Et−Br was graphed (with $R^2 = 0.999$), and the absorption at 285 nm was obtained to assess the degradation. The determination of the limit of detection for the UV−vis instrument involved assessing Et−Br standard concentrations, aiming to establish it at 0.53 μM. The measurements were taken using a 3 mL quartz cuvette. Further, the kinetics rate constant and percentage removal of Et−Br with CAP treatment time were calculated. Fluorescence analysis was determined with a photoluminescence spectrophotometer (QM08075-21-C, Horiba). All irradiation experiments were performed under ambient conditions at a temperature of 25 °C.

2.4. Et−Br Degradation Analysis: HPLC, LC-MS, and FTIR Approaches. We analyzed high-performance liquid chromatography (Agilent 1260 Infinity HPLC) data to monitor changes in the chromatogram to analyze the Et−Br after CAP treatment and the formation of degradation products. There were shifts in retention times, peak intensity changes, or the appearance of new peaks when there was a comparison between control Et−Br and CAP-treated Et−Br. Here, for the HPLC analysis, a Hypersil Gold C-18 (150 mm × 4.6 mm, 3 μ) analytical column was used. Other requirements included a flow rate of 0.6 mL/min and an injection volume of 20 μL at a column oven temperature of 30 ± 0.8 °C. For the mobile phase, acetonitrile was added in double-distilled water in the 50:50 v/v ratio and was detected at 285 nm. Moreover, analyzing liquid chromatography−mass spectrometry (LC/MS) data for the degradation of Et−Br involved assessing the mass spectrometry data to identify the presence of degradation products and monitor changes in their mass-to-charge ratios (m/z) and intensities over time. The Et−Br and degraded products were detected by using a 1200 series LC system (Agilent Technologies, Santa Clara, California), hyphenated to a triple quadrupole (QQQ) mass spectrometer (6470 series, Agilent Technologies) using positive electrospray ionization (+ESI). The mass scan range varied from 50 to 1000 m/z with 10 μL injection volume, a gas temperature of 300 °C, a gas flow of 5 L/min, a 45 psi nebulizer, a sheath gas temperature of 250 °C, a sheath gas flow of 11 L/min, a capillary voltage of 3500 V, and a fragmentor 35V. Moreover, to determine any structural changes in Et−Br before and after CAP treatment, Fourier transform infrared spectroscopy (PerkinElmer Spectrum 2) with attenuated total reflectance (ATR) was performed. The samples were scanned at a resolution of 30 cm^{-1}, and before scanning, the samples were dried in a hot air oven at 50 °C for about 8 h.

2.5. Effects of Et−Br Degradation on Its DNA Intercalation Capacity. Agarose gel electrophoresis is the most widely used method to separate DNA fragments depending on the size. To visualize DNA fragments under UV light, a staining agent is required, which enhances fluorescence after binding with DNA. Although many staining agents are available, Et−Br is widely accepted in biological laboratories. Et−Br interacts with DNA in such a way that it is independent of sequence and intercalates between two adenine−thymine base pairs. In the agarose gel electrophoresis experiment, 1× TAE (Tris-acetate and EDTA) buffer (pH 8) is used to prepare the gel in which Et−Br is added, and then, the gel is illuminated under a Gel Documentation System (GDS) from Chemi DocTM XRS+ (BIO-RAD) to see DNA bands. Even a small concentration of Et−Br is adequate for the intercalation of the DNA, as it forms DNA−Et−Br complexes after binding, which enhance fluorescent yield by 20−30-fold compared to unbound DNA.[29] In this experiment, the nontreated and different exposure time CAP-treated Et−Br (5 mL of 10 μM) is added to the TAE buffer to find out the intercalation ability of Et−Br with bacterial genomic DNA after the CAP treatment. 3 μL of bacterial genomic DNA (50 ng/μL) is loaded into the well of the agarose gel incorporated with treated and nontreated Et−Br. Then, the gel is run for 15 min in the gel electrophoresis system. After the gel electrophoresis, the images are observed, showing the intercalation intensity of the DNA with nontreated and CAP-treated Et−Br by GDS.

2.6. BSA Binding Analyses before and after CAP Treatment. The interaction of Et−Br with BSA was also studied. The BSA stock solution was formulated at a concentration of 5 μM in phosphate buffer solution (PBS) adjusted to a pH of 7.4. All experiments were conducted in triplicate to ensure the precision and reliability of the acquired data. The interaction between Et−Br and BSA was examined by assessing the steady-state fluorescence intensity using a photoluminescence spectrophotometer (model QM08075-21-C, manufactured by Horiba) with excitation at a wavelength of 280 nm. Et−Br exhibits minimal fluorescence at 280 nm. Prior to fluorescence measurements, the BSA−Et−Br complex solution was allowed to incubate for 10 min to ensure adequate interaction. Excitation and emission wavelengths were set at 280 nm and within a range of 200−500 nm,

https://doi.org/10.1021/acsomega.4c04302
ACS Omega 2024, 9, 48044−48054

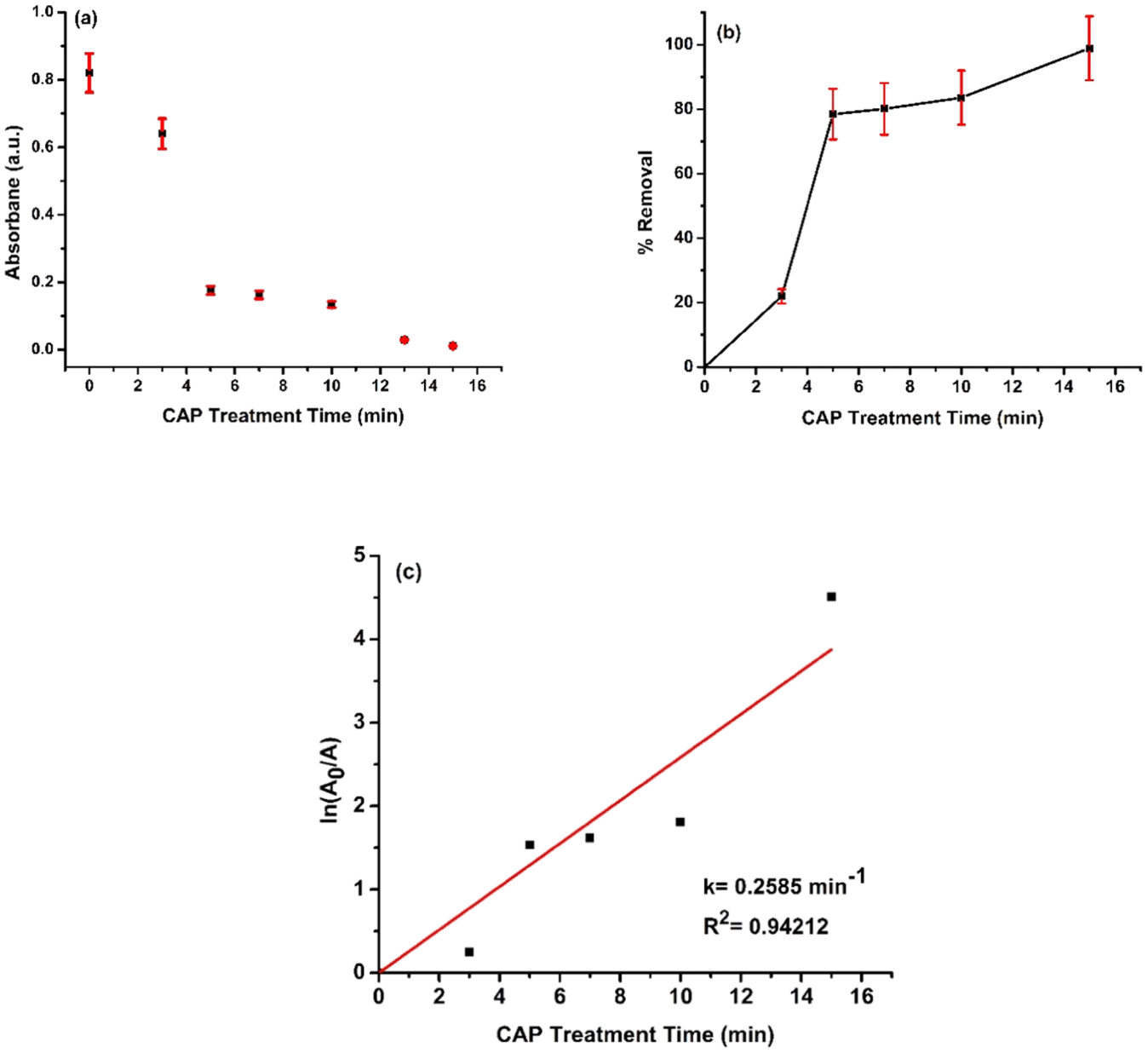

Figure 3. Effect of CAP treatment on Et−Br degradation: (a) absorbance versus CAP treatment time of Et−Br, (b) percentage removal of Et−Br with increasing CAP treatment time, and (c) logarithmic representation of Et−Br degradation as a function of treatment time, fitting the pseudo-first-order kinetics equation.

respectively. A 5 nm slit width was utilized for both excitation and emission spectra.

2.7. Toxicity Experiment. Experiments were conducted to assess the toxicity of Et−Br solutions compared to CAP-treated Et−Br solutions using *E. coli* (ATCC 25922) bacterial growth on agar plates as a qualitative indicator of toxicity. First, *E. coli* was cultured in nutrient broth media and kept at 37 °C under the shaking condition (200 rpm) for 12 h. Then, the culture was serially diluted up to 10^{-6}, and 50 μL of the diluted (10^{-6}) broth culture was spread on the nutrient agar media supplemented with treated and nontreated Et−Br (10 μM) and kept at 37 °C for 12 h, and the appeared CFUs were counted using a colony counter (LAPIZ). To prepare the growth medium, nutrient agar was dissolved in double-distilled water and autoclaved for 20 min at 121 °C. After allowing the mixture to solidify, *E. coli* was streaked on the gel surface and incubated at 37 °C for 24 h to allow *E. coli* to grow. Then, *E. coli* was added to Et−Br, and CAP treated Et−Br (for differen treatment times 5, 10, and 15 min), and was allowed to interact for 1 h. Then, 50 μL of the solution (*E. coli* with Et−Br and CAP treated Et-Br) was transferred to the nutrient agar plate and incubated at 37 °C for 24 h. Quantitative analysis of *E. coli* growth was conducted using a colony counter (LAPIZ).

3. RESULTS AND DISCUSSION

3.1. Generation of Reactive Species in Degradation of Et−Br by CAP. In cold plasma, the AC high-voltage power supply used to accelerate electrons and these high-energy electrons (0.2−2 eV) in the plasma ionizes the He gas via collision, forming electrons, ions, and neutrals.[22−26] The ionization increases the amount of charged particles, which are further accelerated by the electric field, leading to

https://doi.org/10.1021/acsomega.4c04302
ACS Omega 2024, 9, 48044−48054

additional collisions with other atoms and releasing more charged particles.[27−31] Subsequently, electrons gain more energy than ions due to their small mass, and therefore, the temperature of neutrals or ions comparatively is very low than that of electrons.[30,32−35] The charged species produced in the plasma interacts with surrounding air and water vapor molecules on the liquid sample surface are known to produce reactive species ($^{\bullet}OH$, H_2O_2, NO_2, NO_3) by electron impact phenomena, which cause excitation, ionization, and dissociation of the molecules.[36−39] In our previous work, the emission spectra for the He jet were obtained, covering wavelengths from 250 to 900 nm.[15] The presence of various reactive species in the plasma jet can be seen from the spectrum. Also, the presence of the molecular bands in the UV region of the emission spectrum indicates the energetic UV photon emission from the plasma jet.[15,40] Oxidizing OH radicals are also formed in the collision process. The dissociation of water molecules via the electron and metastable collision process produces hydroxyl radicals. The following equations represent the production of OH radicals.

$$e^- + H_2O \rightarrow H^{\bullet} + OH^{\bullet} + e^- \quad (1)$$

$$e^- + He \rightarrow He^* + e^- \quad (2)$$

$$He^* + H_2O \rightarrow OH^{\bullet} + H^{\bullet} + He^* \quad (3)$$

$$He^* + N_2 \rightarrow He + N_2{}^* \quad (4)$$

The presence of singlet oxygen in the spectrum[40] results from collision dissociation of O_2 caused by energetic electrons, and helium metastable is described in eq 5.

$$e^- + O_2 \rightarrow O^{\bullet} + O^{\bullet} + e^- \quad (5)$$

$$N^{\bullet} + OH^{\bullet} \rightarrow NO^{\bullet} + H^{\bullet} \quad (6)$$

$$O^{\bullet} + N^{\bullet} \rightarrow NO^{\bullet} \quad (7)$$

The reactions by excited molecular nitrogen and singlet oxygen, which have enough energy to dissociate water molecules, is represented in the below equations.[39,41]

$$N_2{}^* + H_2O \rightarrow OH^{\bullet} + H^{\bullet} + N_2 \quad (8)$$

$$He^* + N_2 \rightarrow e^- + He + N_2{}^+ \quad (9)$$

$$He^* + O_2 \rightarrow O^{\bullet} + O^{\bullet} + He \quad (10)$$

$$H_2O + O^{\bullet} \rightarrow OH^{\bullet} + OH^{\bullet} \quad (11)$$

3.2. Kinetics Studies of CAP-Treated Et−Br. Et−Br is classified as an immediate or acute hazard according to the regulations outlined in SARA sections 311/312 (40 CFR 370.21).[42] The kinetics of the degradation of Et−Br has been investigated using UV−visible spectroscopy. Absorbance values at λ_{max} = 280 nm were documented for both the control Et−Br and the Et−Br samples treated with CAP at different exposure durations (3, 5, 7, 10, 13, and 15 min).

Absorbance values decrease for Et−Br samples treated with CAP at different exposure durations, as shown in Figure S1. With the increase in the treatment time, the absorbance decreases, as shown in Figure 3(a), and it is well known that the absorbance is the function of the concentration of the solution, and hence, the decrease in the absorbance directly correlates to the decrease in the concentration of Et−Br. Figure 3(b) depicts the percentage removal of Et−Br, and in 15 min, we see approximately 99.99% removal. This indicates CAP's ability to degrade Et−Br and follows a pseudo-first-order reaction, as shown in Figure 3(c). The correlation coefficients (R^2 = 0.94212) suggest a good fit of Et−Br degradation to pseudo-first-order kinetics following eq 12

$$\ln \frac{C}{C_0} = -kt \quad (12)$$

where C and C_0 are the final and initial concentrations of Et−Br, respectively, and k is the kinetic rate constant. From Figure 3(c), k is found to be 0.2585 min^{-1}.

Higher intensities and concentrations of reactive species from CAP are crucial from a treatment standpoint in order to break down organic contaminants.[41,43] A cold plasma produced over the liquid surface in ambient air, as shown in the study of Jaiswal et al., was characterized by FTIR analysis.[41] The presence of different reactive species, such as O_3, NO_2, HNO_2, and others, was discovered to be validated by FTIR during plasma−liquid contact in ambient air.

3.3. Fluorescence Spectra Analysis. The concentration of Et−Br was set as 10 μM, while the excitation wavelength and emission wavelength were, respectively, set as 480 nm and 500−800 nm, with the Et−Br emission maximum at 615 nm.[44] The fluorescence intensity of untreated Et−Br is very high as compared to that of CAP-treated Et−Br, as shown in Figure 4.

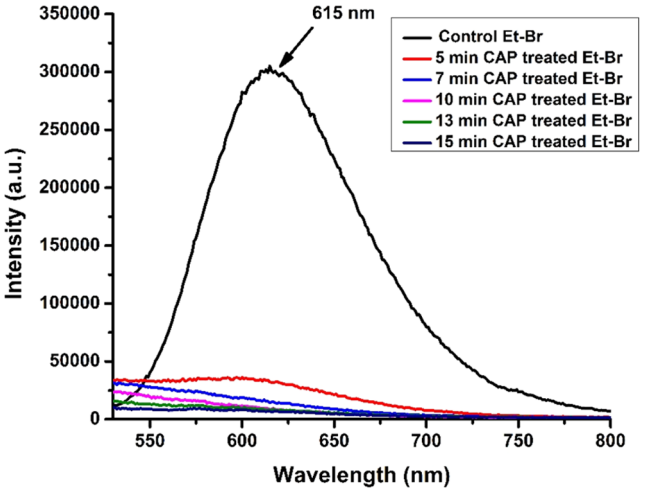

Figure 4. Fluorescence spectrum of control Et−Br and CAP-treated Et−Br.

With CAP treatment of 15 min, the fluorescence intensity almost becomes nil. This indicates that after the CAP treatment, Et−Br undergoes some structural modifications, leading to the quenching of fluorescence intensity. Additionally, we could also see the discoloration of the Et−Br with the CAP treatment (Figure S2). To further understand this, HPLC and LC-MS analyses were carried out.

3.4. HPLC Analysis of CAP-Treated Et−Br. To study the degradation behavior of Et−Br, HPLC was performed. Figure 5 shows the chromatographs of control Et−Br and CAP-treated Et−Br from 3 to 10 min. As shown in Figure 5(a), the major peak at a retention time at 2.934 min has been identified. Et−Br itself has a distinct peak, and degradation byproduct peaks are different, as shown in Figure 5(b−e), for different treatment times.

The changes in retention time, especially the appearance of new peaks, can provide valuable information about the

https://doi.org/10.1021/acsomega.4c04302
ACS Omega 2024, 9, 48044−48054

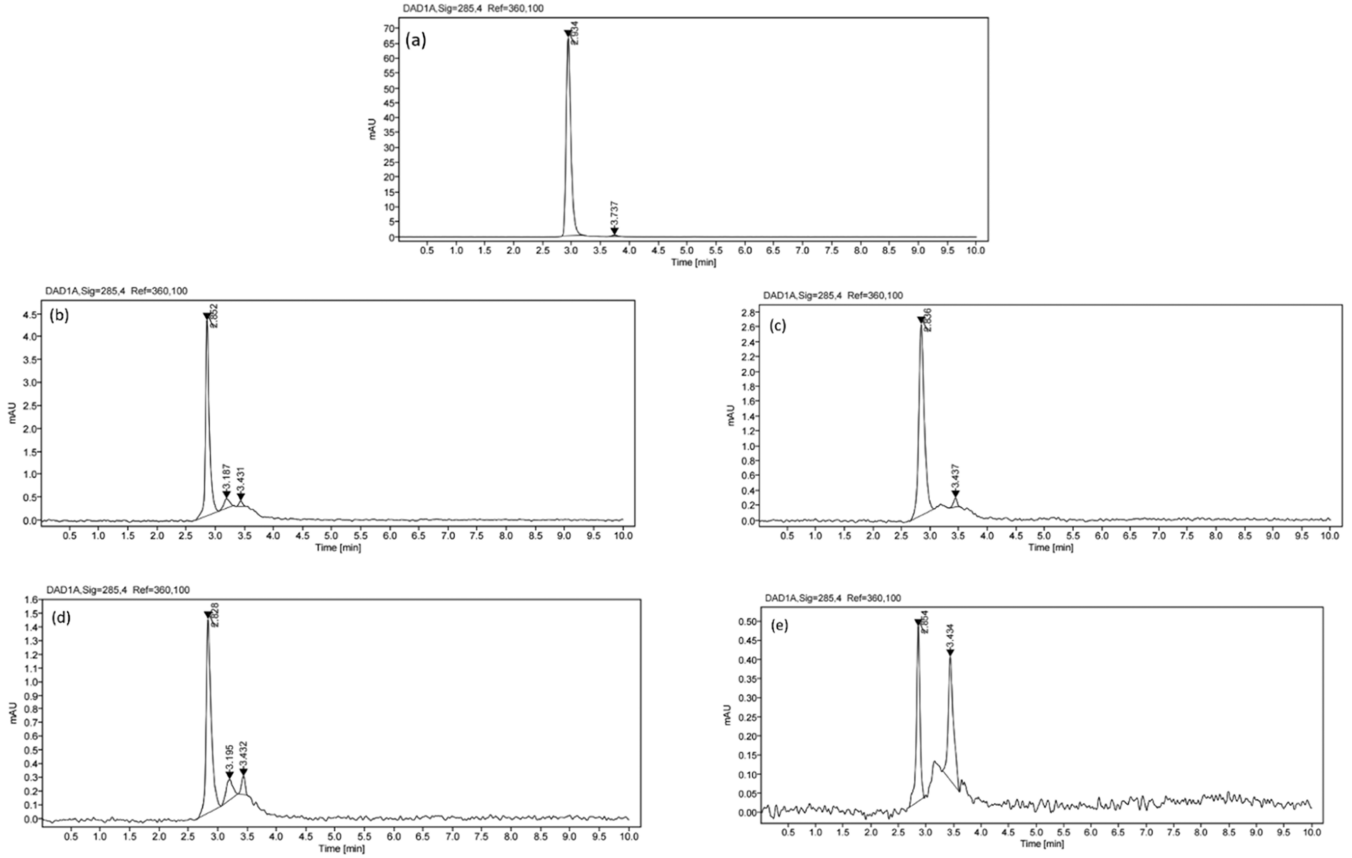

Figure 5. Chromatographs of Et−Br with retention time and peak area: (a) control Et−Br, (b) 3 min CAP-treated Et−Br, (c) 5 min CAP-treated Et−Br, (d) 7 min CAP-treated Et−Br, and (e) 10 min CAP-treated Et−Br.

formation of degradation products or alterations in the chemical composition of a compound. From Figure 5(e), it is clear that 10 min CAP-treated Et−Br breaks down into fragments with retention times of 2.854 and 3.434 min, which signifies the degradation products. Also, it is shown that the detector signal is significantly reduced with an increase in treatment time, which represents the decrease in the concentration of CAP-treated Et−Br. The area under the chromatographic peaks for both Et−Br and any degradation products is also given in Table S1 and provides quantitative data on the concentration of each compound. The percentage area under the peak in Figure 5 has been significantly reduced in comparison with untreated and CAP-treated Et−Br, as given in Table S1. The distinct new peak appears in the chromatograms with respect to the CAP treatment time suggested for further analysis. Further characterization of the degradation products using complementary analytical techniques, LC-MS, and FTIR can help in understanding the specific chemical changes that have taken place after CAP treatment of Et−Br. The FTIR analysis of Et−Br was performed for the control and 10 min CAP-treated Et−Br to verify and supplement information about any change in the compound's chemical structure and functional groups. The characteristic peaks in the region of 1400−1600 cm^{-1} generally correspond to the C=C stretching vibrations of the aromatic rings, which are present in the structure of Et−Br. Et−Br exhibits peaks related to hydrogen bonding interactions, which can be observed in the region of 3000−3500 cm^{-1} (O−H or N−H stretching vibrations). After 15 min CAP, the absence of all of the distinctive FTIR peaks, as shown in Figure S3, confirms the complete degradation of Et−Br.

3.5. LC-MS Analysis of CAP-Treated Et−Br. LC/MS was performed for elucidating the structure of unknown compounds and/or confirming the structure of known ones. Mass spectrometry provides information about the molecular weight, fragmentation patterns, and elemental composition of ions and characterizes structural changes in compounds.

The LC/MS spectra in Figure 6(a) demonstrate the presence of the parent molecule—ethidium ion ($C_{21}H_{20}N_2^+$, m/z 314.15), exhibiting the highest peak (highest intensity) along with some fragmented peaks at m/z 102.14 and 252.08. The LC/MS chromatograms of CAP-treated Et−Br presented in Figure 6(b−f) show the absence of a peak at m/z 314.15 with new peaks, depicting the formation of intermediate products of Et−Br. This could be possible due to the breakdown of the Et−Br molecule into fragments, specifically due to the radicals in CAP attacking and cleaving Et−Br by a ring opening mechanism.[45] We also observe that with CAP treatment of 13 and 15 min, more fragmentation of Et−Br occurs. Such studies on Et−Br were earlier reported using magnetic nanocatalysts and γ irradiation with possible pathways of Et−Br degradation.[14,45]

3.6. Assessment of DNA−Et−Br Binding Interaction after Degradation of Et−Br by CAP. In general, Et−Br is used in gel electrophoresis to visualize the DNA and nucleic acids fragments,[46] due to its ability to bind to the base pairs of DNA, resulting in illumination when viewed under ultraviolet light in the gel image system.[47] The primary binding modes encompass intercalation between base pairs, partial intercala-

https://doi.org/10.1021/acsomega.4c04302
ACS Omega 2024, 9, 48044−48054

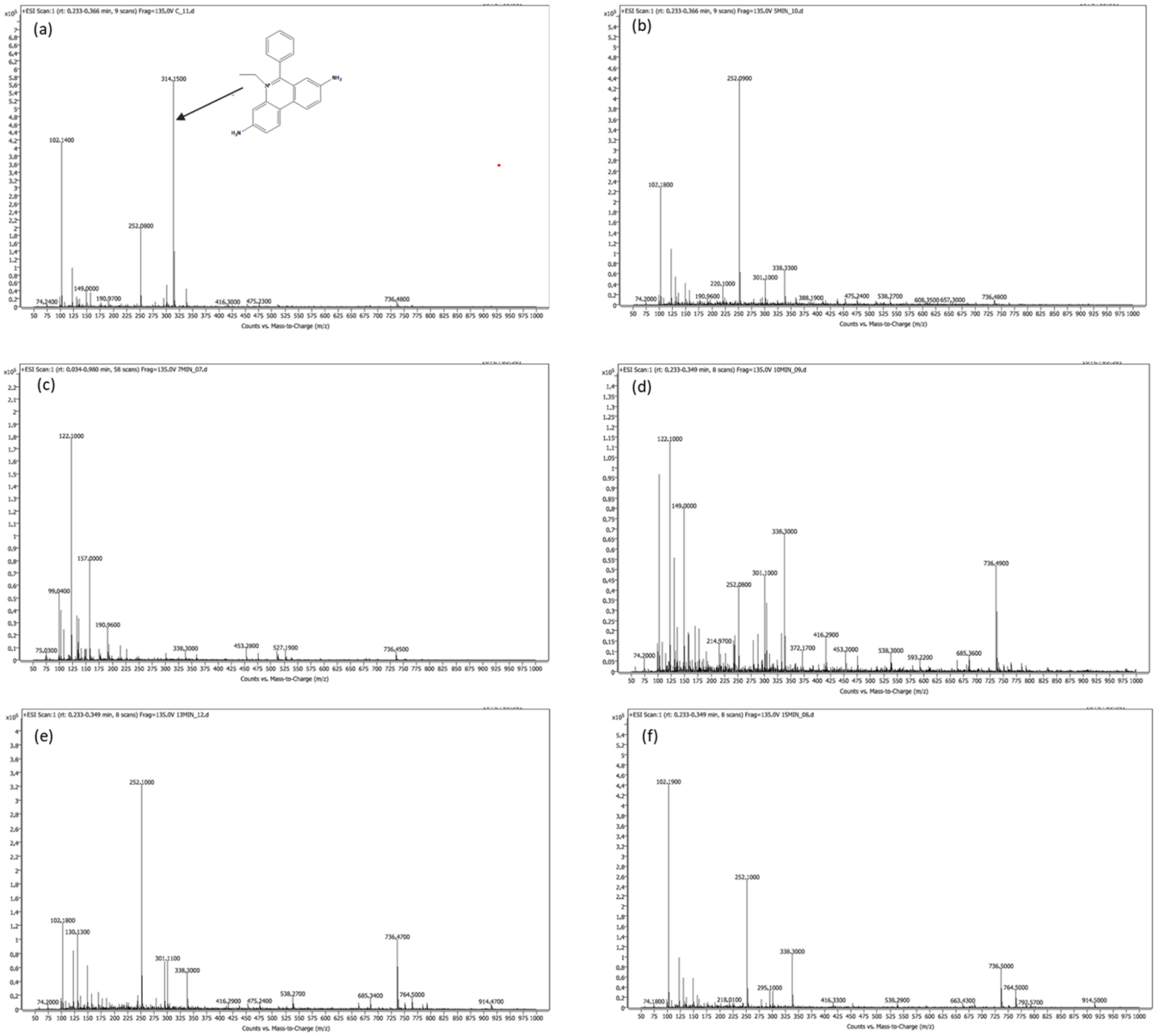

Figure 6. LC/MS spectra of (a) control Et−Br, CAP-treated Et−Br with treatment times of (b) 5 min, (c) 7 min, (d), 10 min, (e) 13 min, and (f) 15 min.

tion, and electrostatic interaction with the DNA phosphate backbone.[48−51] Spectroscopy-based tracking of the ethidium−DNA complex binding kinetics reveals a biphasic binding process. The initial stage involves rapid diffusion of the ligand throughout the DNA polymer, followed by the intercalation event occurring within the millisecond time frame.[52−55]

Here, the TAE buffer was used to make the gel, which was loaded with control Et−Br to visualize DNA, as Et−Br acted as a nonradiative marker to stain DNA. Being a fluorescent dye, the DNA band can be seen clearly under GDS. As shown in Figure 8, the control Et−Br binds with DNA and shows adequate fluorescence. Et−Br interacts with two consecutive base pairs via van der Waals interaction, as it can be inserted perpendicular to the helical axis of the DNA.[56,57] In another set of experiments, CAP-treated Et−Br (5 min) was added to TAE buffer, and Et−Br lost its intercalating ability and fluorescence properties, as shown clearly in Figure 7. This is more explicitly seen with an increase in the CAP treatment time to 10 and 15 min, as shown in Figure 7. CAP-treated Et−Br perturbs the ability to bind to DNA significantly. As elaborated in the preceding section of the paper, the binding ability of CAP-

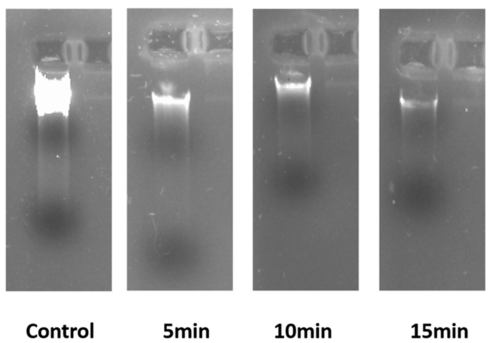

Figure 7. Gel doc image of the gel electrophoresis experiment using nontreated and CAP-treated Et−Br.

https://doi.org/10.1021/acsomega.4c04302
ACS Omega 2024, 9, 48044−48054

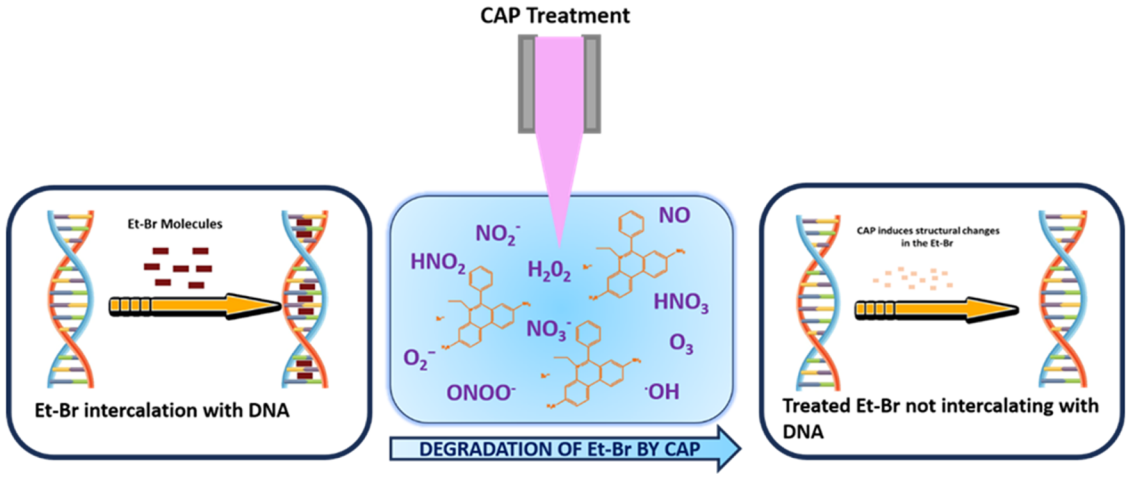

Figure 8. Graphical representation of Et−Br intercalation with DNA before and after CAP treatment.

treated Et−Br to DNA is mainly due to the structural alterations resulting from the ring opening of Et−Br through hydroxylation by the reactive species of CAP. Figure 8 shows a graphical picture of the intercalation of Et−Br with DNA before and after CAP treatment. After Et−Br is degraded by CAP, it ceases to intercalate with DNA, making it non-hazardous to human health and the environment.

3.7. Binding of Et−Br with BSA Analysis before and after CAP Treatment. The interaction between Et−Br and BSA was investigated by analyzing the alteration in intrinsic fluorescence intensity at 330 nm upon excitation at a wavelength of 280 nm. The choice of 280 nm excitation wavelength effectively stimulates the aromatic residues present within BSA. In the absence of Et−Br, BSA demonstrates intrinsic fluorescence emission at 330 nm when excited at 280 nm, primarily contributed by Trp134 and Trp213 residues.[58] Upon addition of Et−Br to BSA, the fluorescence intensity decreases may be due to the change in the conformation of BSA after binding with Et−Br. However, when 5, 10, and 15 min of CAP treated Et−Br was added to BSA, the fluorescence intensity increased significantly as shown in Figure 9. The significant degradation of Et−Br in an aqueous medium results in increased fluorescence intensity, depicting the restoration of the structure of BSA altered in the presence of CAP treated Et−Br.

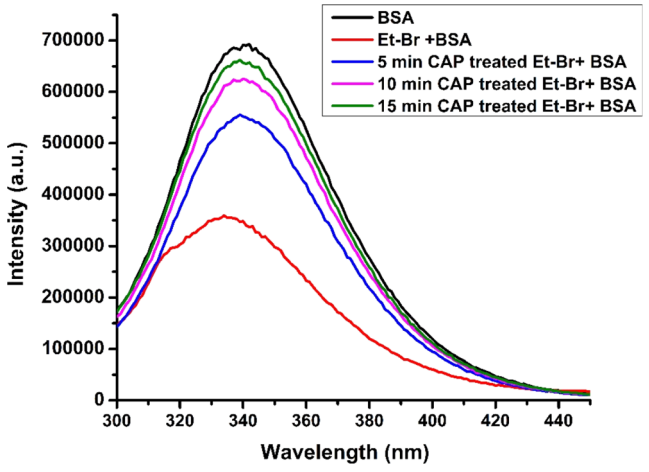

Figure 9. Fluorescence spectrum of control Et−Br and CAP-treated Et−Br binding to BSA.

Additionally, we also performed a detailed binding study of Et−Br with BSA before and after CAP treatment in our work.[59] In conclusion, the degradation of Et−Br results in the inhibition of its binding to BSA, signifying that after CAP treatment, Et−Br residues are not toxic.

3.8. Toxicity Test of the Byproduct of Et−Br after CAP Treatment. Tomchick et al. showed that Et−Br inhibited the growth of *E. coli*.[60] To further elucidate the toxicity of CAP-treated samples, we studied the effect of control Et−Br and CAP-treated Et−Br on *E. coli*. The growth of *E. coli* after exposure to Et−Br is significantly less as compared to the growth observed when *E. coli* is exposed to CAP-treated Et−Br for 5, 10, and 15 min, as shown in Figure 10. As shown in

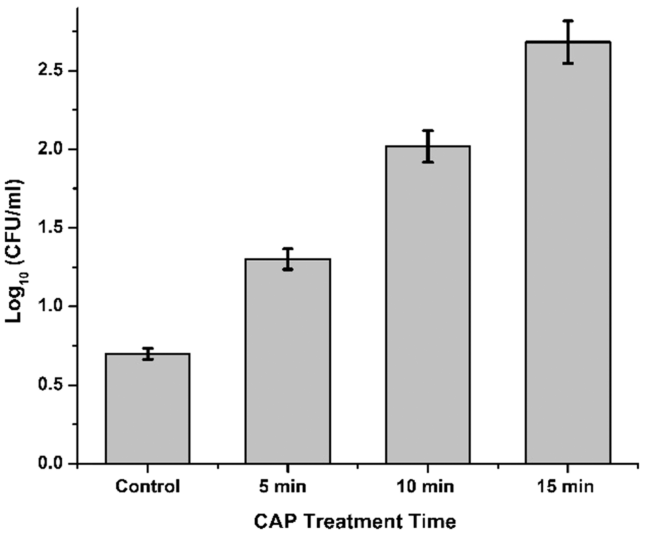

Figure 10. Growth of *E. coli* with Et−Br and 5, 10, and 15 min CAP-treated Et−Br.

Figure S4, CAP treatment can effectively mitigate the toxic effects of Et−Br in increasing the CFU counts and corroborates with the CAP treatment time. Therefore, CAP is a viable alternative technology for protecting the environment, especially with hazardous chemicals such as Et−Br. Furthermore, a comparison of the existing methods to treat

https://doi.org/10.1021/acsomega.4c04302
ACS Omega 2024, 9, 48044−48054

Table 1. Comparison between the Degradation of Et−Br with CAP and Other Methods

S. no.	methods	merits	demerits	references
1.	solution of hypophosphorous acid and sodium nitrite	• inexpensive • reaction mixtures were non-mutagenic	• time-consuming process • solution (hypophosphorous acid and sodium nitrite) is toxic itself • insufficient hypophosphorous acid addition failed to lower the pH below 3, causing the reaction to fail. • produces toxic byproducts	8
2.	adsorption using rectorite and palygorskite	• can adsorb Et−Br from contaminated water without producing secondary toxic products and have large cation exchange capacity and high specific surface area	• need to again thermally destructed inside the interlayer of rectorite • mixed for around 24 h	61,62
3.	adsorb on charcoal filter	• inexpensive • around 90% removal	• cannot be reused • need to mix for one hour for significant removal • incinerate up to 262 °C to destroy Et−Br sorbed on charcoal	63
4.	photocatalytic degradation over TiO_2	• clean light-stimulated degradation • inexpensive • 94% removal	• require around 90 min Et−Br removal with the titania • catalyst products are toxic	9
5.	γ irradiation	• 100% removal • produces no toxic products	• require high dosage to achieve complete degradation	14
6.	CAP	• 100% removal in 15 min • clean and green technology • secondary products are nontoxic	• handling requires expertise	this study

Et−Br is provided in Table 1, highlighting that this study has significant importance in the degradation of harmful chemicals such as Et−Br.

4. CONCLUSIONS

This study demonstrates the effective application of CAP technology for the degradation of Et−Br, addressing both environmental and health concerns associated with its use. The results show that CAP can significantly degrade Et−Br within a short treatment time of 15 min, without the need for additional chemicals and without generating secondary pollutants. The degradation kinetics, following a pseudo-first-order reaction, highlights the efficiency of CAP in this context. Analytical methods, including HPLC and LC-MS, confirm the substantial degradation of Et−Br. Furthermore, toxicity assessments reveal that the degradation products do not intercalate with DNA as well as show less binding with BSA and are nontoxic to *E. coli*, as indicated by increased bacterial growth and CFU counts with increasing CAP treatment time. This study underscores the potential of CAP as a clean, efficient, and environmentally friendly technology for the removal of Et−Br, providing a promising approach to mitigate its environmental and health risks.

■ ASSOCIATED CONTENT

Supporting Information

The Supporting Information is available free of charge at https://pubs.acs.org/doi/10.1021/acsomega.4c04302.

UV spectrum of control Et−Br and 3, 5, 7, 10, 13, and 15 min CAP-treated Et−Br (Figure S1); retention times from HPLC analysis of Et−Br and 3, 5, 7, and 10 min CAP-treated Et−Br (Table S1); Visible discoloration in 15 min CAP-treated Et−Br and FTIR of Et−Br and 15 min CAP-treated Et−Br (Figures S2 and S3); and *E. coli* growth in the presence of Et−Br and 5, 10, and 15 min CAP-treated Et−Br (PDF)

■ AUTHOR INFORMATION

Corresponding Author

Kamatchi Sankaranarayanan − *Physical Sciences Division, Institute of Advanced Study in Science and Technology (An Autonomous Institute Under DST, Govt. of India), Guwahati, Assam 781035, India;* orcid.org/0000-0002-2742-1994; Email: kamatchi.sankaran@gmail.com

Authors

Reema Reema − *Physical Sciences Division, Institute of Advanced Study in Science and Technology (An Autonomous Institute Under DST, Govt. of India), Guwahati, Assam 781035, India; Academy of Scientific and Innovative Research (AcSIR), Ghaziabad, Uttar Pradesh 201002, India*

Tejas Bedmutha − *Physical Sciences Division, Institute of Advanced Study in Science and Technology (An Autonomous Institute Under DST, Govt. of India), Guwahati, Assam 781035, India; Department of Medical Devices, National Institute of Pharmaceutical Education and Research Guwahati (NIPER- G), Guwahati, Assam 781101, India*

Nishanta Kakati − *Physical Sciences Division, Institute of Advanced Study in Science and Technology (An Autonomous Institute Under DST, Govt. of India), Guwahati, Assam 781035, India; Department of Medical Devices, National Institute of Pharmaceutical Education and Research Guwahati (NIPER- G), Guwahati, Assam 781101, India*

Veera Venkata Satya Prasanna Kumari Rayala − *Department of Pharmaceutical Analysis, National Institute of Pharmaceutical Education and Research Guwahati (NIPER- G), Guwahati, Assam 781101, India*

Pullapanthula Radhakrishnanand − *Department of Pharmaceutical Analysis, National Institute of Pharmaceutical Education and Research Guwahati (NIPER-G), Guwahati, Assam 781101, India*

Chingakham Juliya Devi − *Microbial Biotechnology Laboratory, Life Sciences Division, Institute of Advanced Study in Science and Technology, (An Autonomous Institute*

https://doi.org/10.1021/acsomega.4c04302
ACS Omega 2024, 9, 48044−48054

Under DST, Govt. of India), Guwahati, Assam 781035, India

Debajit Thakur − *Microbial Biotechnology Laboratory, Life Sciences Division, Institute of Advanced Study in Science and Technology, (An Autonomous Institute Under DST, Govt. of India), Guwahati, Assam 781035, India*

Complete contact information is available at: https://pubs.acs.org/10.1021/acsomega.4c04302

Notes

The authors declare no competing financial interest.

■ ACKNOWLEDGMENTS

This work was supported by ICMR Project grant (File No. 17x(3)/Ad-hoc/19/2022-ITR dt. 23.12.2022), DST-IASST, Guwahati In-house project grant, and SRG grant (SRG/2020/001894 dt. 11.11.2020). Reema thanks UGC and AcSIR for the fellowship and PhD registration. The authors thank SAIC and IASST for the instrumentation facilities.

■ REFERENCES

(1) Stothard, J. R.; Frame, I. A.; Miles, M. A. An evaluation of four staining methods for the detection of DNA in nondenaturing polyacrylamide gels. *Anal. Biochem.* **1997**, *253* (2), 262−264.

(2) Cariello, N. F.; Keohavong, P.; Sanderson, B. J.; Thilly, W. G. DNA damage produced by ethidium bromide staining and exposure to ultraviolet light. *Nucleic Acids Res.* **1988**, *16* (9), No. 4157.

(3) Waring, M. J. Complex formation between ethidium bromide and nucleic acids. *J. Mol. Biol.* **1965**, *13* (1), 269−282.

(4) Macgregor, J. T.; Johnson, I. J. In vitro metabolic activation of ethidium bromide and other phenanthridinium compounds: mutagenic activity in Salmonella typhimurium. *Mutat. Res.* **1977**, *48* (1), 103−107. 1977.

(5) Amirijavid, S.; Mohammadi, M. Toxicity of the ethidium bromide on germination of wheat, alfalfa and tomato. *Inter. Invention J. Agri. Soil Sci.* **2014**, *2* (5), 69−74.

(6) Singer, V. L.; Lawlor, T. E.; Yue, S. Comparison of SYBR Green I nucleic acid gel stain mutagenicity and ethidium bromide mutagenicity in the Salmonella/mammalian microsome reverse mutation assay (Ames test). *Mutat. Res., Genet. Toxicol.* **1999**, *439* (1), 37−47.

(7) Singh, S.; Singh, A. N. Ethidium bromide: Is a stain turning into a pollutant? A synthesis on its status, waste management, monitoring challenges and ecological risks to the environment. *Int. J. Res. Anal. Rev.* **2018**, *4*, 226−233.

(8) Lunn, G.; Sansone, E. B. Ethidium bromide: destruction and decontamination of solutions. *Anal. Biochem.* **1987**, *162* (2), 453−458.

(9) Adán, C.; Martínez-Arias, A.; Fernández-García, M.; Bahamonde, A. Photocatalytic degradation of ethidium bromide over titania in aqueous solutions. *Appl. Catal., B* **2007**, *76* (3−4), 395−402.

(10) Zhang, C.; Liu, L.; Wang, J.; Rong, F.; Fu, D. Electrochemical degradation of ethidium bromide using boron-doped diamond electrode. *Sep. Purif. Technol.* **2013**, *107*, 91−101.

(11) Klein, J.; Waldvogel, S. R. Selective Electrochemical Degradation of Lignosulfonate to Bio-Based Aldehydes. *ChemSusChem* **2023**, *16* (8), No. 202202300.

(12) Gandhi, V. P.; Kesari, K. K.; Kumar, A. The identification of ethidium bromide-degrading bacteria from laboratory gel electrophoresis waste. *BioTech* **2022**, *11* (1), 4.

(13) Wang, M.; Wen, J.; Huang, Y.; Hu, P. Selective Degradation of Styrene-Related Plastics Catalyzed by Iron under Visible Light. *ChemSusChem* **2021**, *14* (22), 5049−5056.

(14) Alnajrani, M. N.; Alsager, O. A. Decomposition of DNA staining agent ethidium bromide by gamma irradiation: Conditions, kinetics, by-products, biological activity, and removal from wastewater. *J. Hazard. Mater. Adv.* **2020**, *389*, No. 122142.

(15) Khanikar, R. R.; Kalita, M.; Kalita, P.; Kashyap, B.; Das, S.; Khan, M. R.; Bailung, H.; Sankaranarayanan, K. Cold atmospheric pressure plasma for attenuation of SARS-CoV-2 spike protein binding to ACE2 protein and the RNA deactivation. *RSC Adv.* **2022**, *12* (15), 9466−9472.

(16) Sanito, R. C.; You, S. J.; Wang, Y. F. Degradation of contaminants in plasma technology: An overview. *J. Hazard. Mater. Adv.* **2022**, *424*, No. 127390.

(17) Takeuchi, N.; Yasuoka, K. Review of plasma-based water treatment technologies for the decomposition of persistent organic compounds. *Jpn. J. Appl. Phys.* **2020**, *60*, No. 0801.

(18) Laroussi, M. Cold plasma in medicine and healthcare: The new frontier in low temperature plasma applications. *Front. Phys.* **2020**, *8*, No. 74.

(19) Basumatary, D.; Bailung, H.; Sankaranarayanan, K. Comparative Analysis of Direct Cold Atmospheric Plasma Treatment vs. Plasma Activated Water for the Deactivation of Omicron Variant of SARS-CoV-2. *Plasma Chem. Plasma Process.* **2024**, *44*, 1−12.

(20) Kovačič, A.; Modic, M.; Hojnik, N.; Vehar, A.; Kosjek, T.; Heath, D.; Walsh, J. L.; Cvelbar, U.; Heath, E. Degradation of bisphenol A and S in wastewater during cold atmospheric pressure plasma treatment. *Sci. Total Environ.* **2022**, *837*, No. 155707.

(21) Brisset, J. L.; Fanmoe, J.; Hnatiuc, E. Degradation of surfactant by cold plasma treatment. *J. Environ. Chem. Eng.* **2016**, *4* (1), 385−387.

(22) Hijosa-Valsero, M.; Molina, R.; Montràs, A.; Müller, M.; Bayona, J. M. Decontamination of waterborne chemical pollutants by using atmospheric pressure nonthermal plasma: a review. *Environ. Technol. Rev.* **2014**, *3* (1), 71−91.

(23) Malik, M. A. Water purification by plasmas: Which reactors are most energy efficient? *Plasma Chem. Plasma Process.* **2010**, *30*, 21−31.

(24) Dey, A.; Rasane, P.; Choudhury, A.; Singh, J.; Maisnam, D.; Rasane, P. Cold plasma processing: A review. *Res. J. Pharm., Biol. Chem. Sci.* **2016**, *9* (4), 2980−2984.

(25) Lukes, P.; Dolezalova, E.; Sisrova, I.; Clupek, M. Aqueous-phase chemistry and bactericidal effects from an air discharge plasma in contact with water: evidence for the formation of peroxynitrite through a pseudo-second-order post-discharge reaction of H2O2 and HNO2. *Plasma Sources Sci. Technol.* **2014**, *23* (1), No. 015019.

(26) Khanikar, R. R.; Boruah, P. J.; Bailung, H. Development and optical characterization of an atmospheric pressure non-thermal plasma jet for superhydrophobic surface fabrication. *Plasma Res. Express* **2020**, *2* (4), No. 045002.

(27) Bruggeman, P.; Brandenburg, R. Atmospheric pressure discharge filaments and microplasmas: physics, chemistry and diagnostics. *J. Phys. D: Appl. Phys.* **2013**, *46* (46), No. 464001.

(28) Kumar, A.; Škoro, N.; Gernjak, W.; Jovanović, O.; Petrović, A.; Živković, S.; Lumbaque, E. C.; Farré, M. J.; Puač, N. Degradation of diclofenac and 4-chlorobenzoic acid in aqueous solution by cold atmospheric plasma source. *Sci. Total Environ.* **2023**, *864*, No. 161194.

(29) Bradu, C.; Kutasi, K.; Magureanu, M.; Puač, N.; Živković, S. Reactive nitrogen species in plasma-activated water: Generation, chemistry and application in agriculture. *J. Phys. D: Appl. Phys.* **2020**, *53* (22), No. 223001.

(30) LePecq, J. B.; Paoletti, C. A fluorescent complex between ethidium bromide and nucleic acids: physical—chemical characterization. *J. Mol. Biol.* **1967**, *27* (1), 87−106.

(31) Bruggeman, P. J.; Kushner, M. J.; Locke, B. R.; Gardeniers, J. G.; Graham, W. G.; Graves, D. B.; Hofman-Caris, R.C.H.M.; Maric, D.; Reid, J. P.; Ceriani, E.; Rivas, D. F.; et al. Plasma−liquid interactions: a review and roadmap. *Plasma Sources Sci. Technol.* **2016**, *25* (5), No. 053002.

(32) Foster, J.; Sommers, B. S.; Gucker, S. N.; Blankson, I. M.; Adamovsky, G. Perspectives on the interaction of plasmas with liquid water for water purification. *IEEE Trans. Plasma Sci.* **2012**, *40* (5), 1311−1323. 2012.

(33) Attri, P.; Yusupov, M.; Park, J. H.; Lingamdinne, L. P.; Koduru, J. R.; Shiratani, M.; Choi, E. H.; Bogaerts, A. Mechanism and comparison of needle-type non-thermal direct and indirect atmospheric pressure plasma jets on the degradation of dyes. *Sci. Rep.* **2016**, *6* (1), No. 34419.
(34) Mouele, E. S. M.; Tijani, J. O.; Fatoba, O. O.; Petrik, L. F. Degradation of organic pollutants and microorganisms from wastewater using different dielectric barrier discharge configurations—a critical review. *Environ. Sci. Pollut. Res.* **2015**, *22*, 18345−18362.
(35) Jiang, B.; Zheng, J.; Qiu, S.; Wu, M.; Zhang, Q.; Yan, Z.; Xue, Q. Review on electrical discharge plasma technology for wastewater remediation. *Chem. Eng. J.* **2014**, *236*, 348−368.
(36) Schiorlin, M.; Paradisi, C.; Brandenburg, R.; Schmidt, M.; Marotta, E.; Giardina, A.; Basner, R.Pollutant degradation in gas streams by means of non-thermal plasmas. In *Current Air Quality Issues*; Farhad Nejadkoorki, 2015; pp 4−34.
(37) García, M. C.; Mora, M.; Esquivel, D.; Foster, J. E.; Rodero, A.; Jiménez-Sanchidrián, C.; Romero-Salguero, F. J. Microwave atmospheric pressure plasma jets for wastewater treatment: degradation of methylene blue as a model dye. *Chemosphere* **2017**, *180*, 239−246.
(38) Yehia, S. A.; Zarif, M. E.; Bita, B. I.; Teodorescu, M.; Carpen, L. G.; Vizireanu, S.; Petrea, N.; Dinescu, G. Development and optimization of single filament plasma jets for wastewater decontamination. *Plasma Chem. Plasma Process.* **2020**, *40* (6), 1485−1505.
(39) Invernizzi, L.; Muja, C.; Sainct, F. P.; Guillot, P. Investigation of RONS production and complex molecules degradation induced by an APPJ generated by two different sources. *IEEE Trans. Radiat. Plasma Med. Sci.* **2020**, *4* (1), 121−129.
(40) Reema, K. R.; Bailung, H.; Sankaranarayanan, K. Review of the cold atmospheric plasma technology application in food, disinfection, and textiles: A way forward for achieving circular economy. *Front. Phys.* **2022**, *10*, No. 942952.
(41) Jaiswal, S.; Aguirre, E. M. Comparison of atmospheric pressure argon producing O (1S) and helium plasma jet on methylene blue degradation. *AIP Adv.* **2021**, *11* (4), No. 045311, DOI: 10.1063/5.0046948.
(42) Maccs, K. U.S. Environmental Protection Agency. *Toxics Release Inventory (TRI) Program*; MDL Information Systems, Inc.: San Leandro, CA. https://www.epa.gov/toxics-release-inventory-tri-program (accessed 2019-02-21), 1984.
(43) Naz, M. Y.; Shukrullah, S.; Rehman, S. U.; Khan, Y.; Al-Arainy, A. A.; Meer, R. Optical characterization of non-thermal plasma jet energy carriers for effective catalytic processing of industrial wastewaters. *Sci. Rep.* **2021**, *11* (1), No. 2896.
(44) Sabnis, R. W. *Handbook of Biological Dyes and Stains: Synthesis and Industrial Applications*. John Wiley & Sons 2010.
(45) Xie, E.; Zheng, L.; Ding, A.; Zhang, D. Mechanisms and pathways of ethidium bromide Fenton-like degradation by reusable magnetic nanocatalysts. *Chemosphere* **2021**, *262*, No. 127852.
(46) Sigmon, J.; Larcom, L. L. The effect of ethidium bromide on mobility of DNA fragments in agarose gel electrophoresis. *Electrophoresis* **1996**, *17* (10), 1524−1527.
(47) Lee, P. Y.; Costumbrado, J.; Hsu, C. Y.; Kim, Y. H. Agarose gel electrophoresis for the separation of DNA fragments. *J. Visualized Exp.* **2012**, No. 62, No. 3923.
(48) Porschke, D. Time-resolved analysis of macromolecular structures during reactions by stopped-flow electrooptics. *Biophys. J.* **1998**, *75* (1), 528−537.
(49) Baranovskii, S. F.; Chernyshev, D. N.; Buchel'nikov, A. S.; Evstigneev, M. P. Thermodynamic analysis of complex formation of ethidium bromide with DNA in water solutions. *Biophysics* **2011**, *56*, 214−219.
(50) Vardevanyan, P. O.; Antonyan, A. P.; Hambardzumyan, L. A.; Shahinyan, M. A.; Karapetian, A. T. Thermodynamic analysis of DNA complexes with methylene blue, ethidium bromide and Hoechst 33258. *Biopolym. Cell* **2013**, *29* (6), 515−520.
(51) Vardevanyan, P. O.; Arakelyan, V. B.; Parsadanyan, M. A.; Antonyan, A. P.; Hovhannisyan, G. G.; Shahinyan, M. A. Analysis of experimental binding curves of EtBr with single-and double-stranded DNA at small fillings. *Mod. Phys. Lett. B.* **2014**, *28* (22), No. 1450178.
(52) Vardevanyan, P. O.; Antonyan, A. P.; Parsadanyan, M. A.; Torosyan, M. A.; Karapetian, A. T. Joint interaction of ethidium bromide and methylene blue with DNA. The effect of ionic strength on binding thermodynamic parameters. *J. Biomol. Struct. Dyn.* **2016**, *34* (7), 1377−1382.
(53) Wakelin, L. P. G.; Waring, M. J. Kinetics of drug-DNA interaction: dependence of the binding mechanism on structure of the ligand. *J. Mol. Biol.* **1980**, *144* (2), 183−214.
(54) Li, H. J.; Crothers, D. M. Relaxation studies of the proflavine-DNA complex: the kinetics of an intercalation reaction. *J. Mol. Biol.* **1969**, *39* (3), 461−477. 1969.
(55) Porumb, H. The solution spectroscopy of drugs and the drug-nucleic acid interactions. *Prog. Biophys. Mol. Biol.* **1979**, *34*, 175−195.
(56) Galindo-Murillo, R.; Cheatham, T. E., III Ethidium bromide interactions with DNA: an exploration of a classic DNA−ligand complex with unbiased molecular dynamics simulations. *Nucleic Acids Res.* **2021**, *49* (7), 3735−3747.
(57) Green, M. R.; Sambrook, J. Polymerase chain reaction. *Cold Spring Harbor Protoc.* **2019**, *2019* (6), No. pdb-top095109, DOI: 10.1101/pdb.top095109.
(58) Jeremias, H. F.; Lousa, D.; Hollmann, A.; Coelho, A. C.; Baltazar, C. S.; Seixas, J. D.; Marques, A. R.; Santos, N. C.; Romao, C. C.; Soares, C. M. Study of the interactions of bovine serum albumin with a molybdenum (II) carbonyl complex by spectroscopic and molecular simulation methods. *PLoS One* **2018**, *13* (9), No. 0204624.
(59) Kakati, N.; Radhakrishnanand, P.; Sankaranarayanan, K. Insights on Cold Atmospheric Plasma Treatment of Ethidium Bromide and its Binding to protein BSA. *Phys. Scr.* **2014**, *99* (9), No. 095609.
(60) Tomchick, R.; Mandel, H. G. Biochemical effects of ethidium bromide in micro-organisms. *Microbiology* **1964**, *36* (2), 225−236.
(61) Chang, P. H.; Sarkar, B. Mechanistic insights into ethidium bromide removal by palygorskite from contaminated water. *J. Environ. Manage.* **2021**, *278*, No. 111586.
(62) Li, Z.; Chang, P. H.; Jiang, W. T.; Liu, Y. Enhanced removal of ethidium bromide (EtBr) from aqueous solution using rectorite. *J. Hazard. Mater.* **2020**, *384*, No. 121254. 2020.
(63) Novania, S.; Widagdo, A. R. P.; Prihatiningrum, D. M.; Fauziyah, S.; Sucipto, T. H. Ethidium Bromide Waste Treatment with Activated Charcoal. *EnvironmentAsia* 2023, *16*, 138.

https://doi.org/10.1021/acsomega.4c04302
ACS Omega 2024, 9, 48044−48054